IEEE Photonics Journal
An IEEE Photonics Society Publication

Open Access

Joint Influence of the Optical Carrier-to-Sideband Ratio and Guard Band on Direct-Detection SSB-OOFDM System

Volume 7, Number 5, October 2015

Jianxin Ma
Wei Zhou

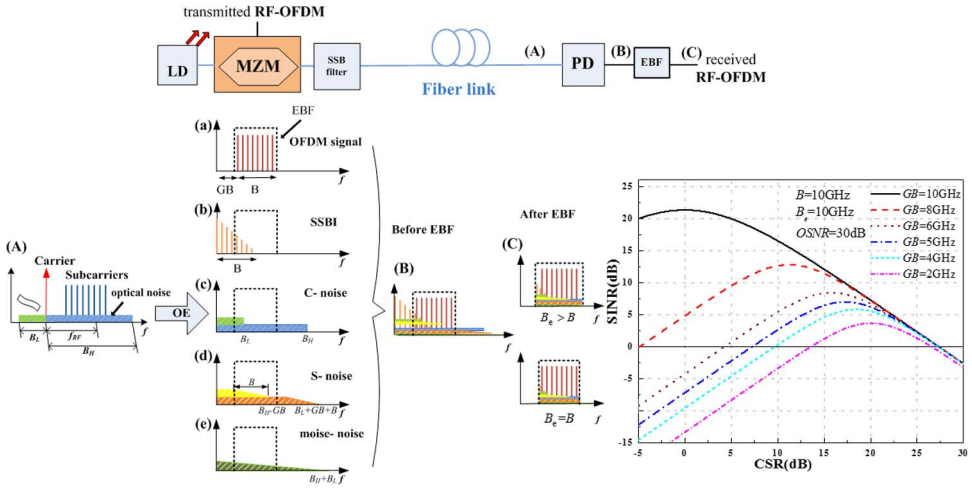

DOI: 10.1109/JPHOT.2015.2470130
1943-0655

Joint Influence of the Optical Carrier-to-Sideband Ratio and Guard Band on Direct-Detection SSB-OOFDM System

Jianxin Ma and Wei Zhou

State Key Laboratory of Information Photonics and Optical Communications, School of Electronic Engineering, Beijing University of Posts and Telecommunications, Beijing 100876, China

DOI: 10.1109/JPHOT.2015.2470130

Manuscript received August 8, 2015; accepted August 17, 2015. Date of current version September 8, 2015. This work was supported by Fund of State Key Laboratory of Information Photonics and Optical Communications (Beijing University of Posts and Telecommunications), P. R. China. Corresponding author: J. Ma (e-mail: majianxinxy@163.com).

Abstract: The signal-to-interference-plus-noise ratio of the noised single-sideband optical orthogonal frequency-division multiplexing (SSB-OOFDM) signal in a direct-detection OFDM system is first deduced theoretically. The relationship of the carrier-to-sideband ratio (CSR) and guard band (GB) to the signal-to-signal beat interference (SSBI) is explored. According to our theoretical analysis, the degradation caused by SSBI on the SSB-OOFDM signal becomes worse as the GB reduces, whereas the increase in the CSR can loosen this degradation. Therefore, a tradeoff between the GB and CSR balances their joint influence on system performance. The simulation for the 20-km optical link with 40-Gb/s 16-quadrature amplitude modulation (16-QAM) noised SSB-OOFDM signal is conducted to confirm our theoretical results. It shows that, without any complex device or algorithm, the GB can be reduced to 40% only by increasing the CSR to ~8 dB, and thus, the spectral efficiency of the DDO-OFDM link is improved after optimizing the CSR and GB of the SSB-OOFDM signal. In addition, the influence of the optical signal-to-noise ratio and the electronic filter on the optimum CSR of the system is further analyzed.

Index Terms: Direct-detection SSB-OOFDM, carrier-to-sideband ratio, signal-to-signal beat interference.

1. Introduction

Orthogonal frequency division multiplexing (OFDM) has high spectral efficiency and robustness to inter-symbol interference (ISI) in the wireless communication, but it did not attract much attention due to the implement complexity until the appearance of the digital signal processing technology and large scale integration, which makes it more effective to achieve high speed modulation and demodulation via forward and inverse fast Fourier transform (FFT/IFFT) in communication systems. It greatly reduces the implementation complexity and application costs of the OFDM technology. Since 2006, optical OFDM (OOFDM) technology has also got extensive researches in high speed optical transmission system due to its high spectral efficiency (SE), dynamic bandwidth allocation and powerful anti-dispersion property. It can be mainly classified as coherent optical OFDM (CO-OFDM) and direct-detection optical OFDM (DDO-OFDM). CO-OFDM is suitable for long-haul optical transmission due to its high spectral efficiency, receiver sensitivity, and great robustness against both chromatic and polarization dispersion. However,

narrow linewidth lasers are required at both transmitter and receiver, and extra signal processing is needed to solve the phase noise and frequency offset. DDO-OFDM has been proposed for lowering the cost and complexity of the receiver in that only a square-law photodiode (PD) is required at receiver to convert the optical signal to the electrical one. The phase and frequency offset can be cancelled out because the OOFDM signal and the optical carrier come from the same laser with the synchronous frequency and the phase offset [1]–[4], and therefore, the laser linewidth of the transmitter is loosened greatly. Therefore, DDO-OFDM is regarded as a promising candidate for the optical access net for its advantages of simple configuration and low cost.

There are many works reported on the DDO-OFDM technology [2]–[26]. Although directly modulated laser or double sideband external modulation with direction detection is a cost-effective implement for the optical access network, its intersubcarrier interference and high frequency-selective attenuation need to be overcome due to its double sideband spectrum [5], [6]. To solve these issues, adaptive code rate technique, pre-emphasis technique and pilot aided estimation are proposed [4]–[17]. In [7], [8], Cao *et al.* had analyzed the intersubcarrier interference and frequency-selective fading of the DDO-OFDM system without guard band (GB), and Turbo codes and bit interleaver technologies were proposed to mitigate their degradation. SSB-OOFDM signal can overcome the periodical power fading effect associated with double-sideband OOFDM signal with improved SE [4], [9]. In [10], Lowery had presented the generation mechanism of the beating noises of the OFDM signal in the process of the optical/electrical conversion with enough GB to avoid the degradation of the signal-signal beat interference (SSBI), and the influence of ASE noise is also analyzed.

In general, the SSB-OOFDM systems with a minimum GB equal to the bandwidth of the SSB-OOFDM signal (B) can make the SSBI and desired RF spectra nonoverlapping and the system gets the best receiver sensitivity at the carrier to sideband (CSR) of 0 dB [18] while the SE is only half of that in the CO-OFDM system [1]. The SE of the SSB- OOFDM system can be enhanced further by reducing the GB but at the expense of increasing distortion of the SSBI. Many research works [3], [4], [7], [8], [19]–[22] attempted to minimize the penalty due to SSBI with an improved SE. Pairing subcarrier [3], iterative technique [8], adaptive modulation technique [19], training sequence [20], and half-cycled OFDM [21] were proposed to suppress the SSBI of the SSB-OOFDM signal with reduced GB. A recently proposed balanced detection at the receiver front can effectively eliminate the SSBI and discard the GB, which doubles the SE in a typical DDO-OFDM system [4], [22], but a more complicated receiver or algorithm for signal processing is required to achieve higher spectral efficiency and receiver sensitivity.

According to the direct-detection SSB-OOFDM system without GB in [9], a large CSR about 14 dB could suppress the degradation caused by the SSBI greatly. In addition, Lowery has proposed a scheme to suppress the SSBI by boosting the optical carrier level relative to the optical OFDM signal at receiver, and thus the GB can be reduced without SSBI penalty [17]. Jansen *et al.* found that there is a tradeoff between the ASE noise and SSBI since the impact of ASE noise is dominant for SSB-OOFDM signal with higher CSR [24]. However, the higher main optical carrier would also yield a poorer sensitivity and lower power efficiency since the optical carrier with more power bears no information. In [25], Ali *et al.* also found that biasing Mach–Zehnder modulator (MZM) at the quadrature point resulted in a significant reduction of SSBI. By this way, the GB can be reduced at least 50%.

From the above, we believe that, both CSR and GB of the SSB-OOFDM signal have influence on the SSBI of the DDO-OFDM system in a joint pattern in intuition. Although, many researches on each aspect have been reported in the literature, and SSBI model has been established well for optical OFDM with many schemes and DSP algorithms to solve the SSBI, their joint influence on the link performance of the direct-detection SSB-OOFDM system has not been studied systemically to our best knowledge. In this paper, we have theoretically analyzed the mechanism of the influence of the SSBI on the DD-OFDM system with noised optical SSB-OOFDM signal in terms of both CSR and GB in details, which will be a meaningful and deeper exploration to improve the SE in DDO-OFDM with GB $< B$. Here the influence of the GB, optical signal to noise ratio (OSNR) and electronic bandpass filters (EBF) on the optimum CSR is further

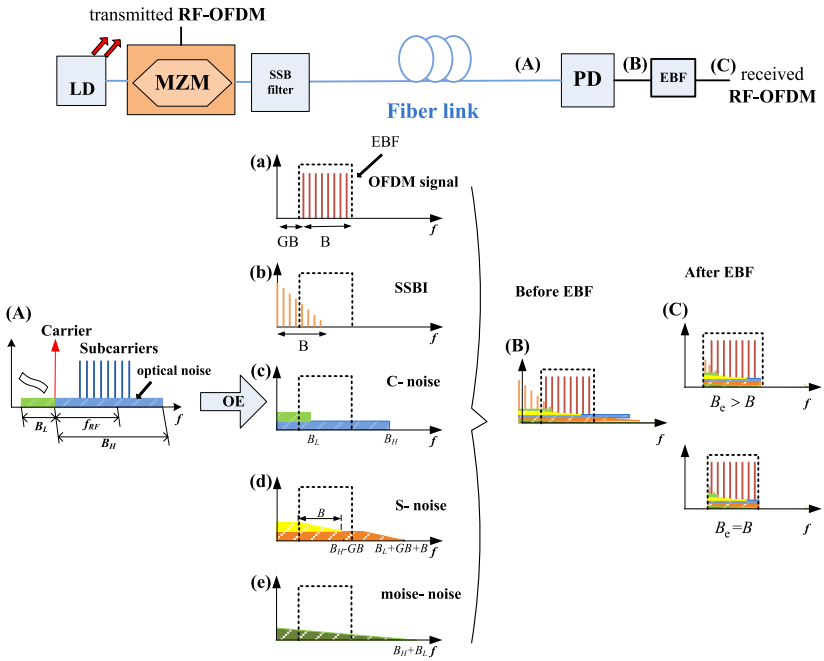

Fig. 1. SSB-OOFDM link with direct detection and principle of the opto-electrical conversion of the noised SSB-OOFDM signal in frequency domain, including the optical SSB-OOFDM spectrum, its beating results of different components in the electrical domain, and the results before and after a EBF.

explored. Moreover, the tradeoff between GB and CSR is balanced. To verify our analysis, the simulation with a direct-detection SSB-OOFDM transmission link is built with the 40 Gb/s 16-quadrature amplitude modulation (QAM) SSB-OOFDM signal. The simulation results demonstrate that the increase of the error vector magnitude (EVM) caused by the reduced GB, improving SE of the system, can be compensated for by simply increasing the CSR in some degree. The simulation results show that without any complex device or algorithm, the GB can be reduced to 40% only by increasing the CSR to ~8 dB, and so the SE of the DDO-OFDM link is improved after optimizing the CSR and GB of the transmitted SSB-OOFDM signal. These agree well with our theoretical analysis. Based on the trade-off between the CSR and GB of the noised SSB-OOFDM signal with a given optical power, we can obtain the optimal link performance of the direct-detection SSB-OOFDM link with higher SE and higher power efficiency, which is valuable for the design of the DDO-OFDM system. The DDO-OFDM link after optimizing the performance by the optical CSR and GB of the SSB-OOFDM signal is an excellent candidate for short-reach and metropolitan optical transmissions due to its high SE and receive sensitivity with simple and cost-efficient receiver.

This paper is arranged as follows: the interaction mechanism of the SSBI on the received OFDM signal from the noised SSB-OOFDM signal is described theoretically, the analytical expression of signal to interference plus noise ratio (SINR) of the received electrical OFDM signal is derived mathematically and SINR versus CSR, GB, and OSNR at different bandwidth of the EBF (B_e) is analyzed in Section 2. Then, to verify our theoretical results, in Section 3, a simulation link of direct-detection SSB-OOFDM transmission system with the SSB-OOFDM signal is built, and the simulation results are further analyzed and discussed in detail. Finally, conclusions are drawn in Section 4.

2. SSBI and Noise of OFDM Signal Detected From the Noised SSB-OOFDM Signal With Reduced GB

Fig. 1 shows a SSB-OOFDM link with direct detection and principle of the opto-electrical conversion of the noised SSB-OOFDM signal in frequency domain. The SSB-OOFDM signal can be

generated by optical single-sideband modulation of RF-OFDM, optical double-sideband modulation of RF-OFDM with optical SSB filtering, or optical modulation of a baseband OFDM signal and addition of an optical carrier. Generally, the noised SSB-OOFDM signal can be expressed as

$$\begin{aligned}\mathbf{E}_0(t) =& \mathbf{E}_{C0}e^{j2\pi f_0 t} + \mathbf{E}_{S0}s_B(t)e^{j2\pi(f_0+f_{\mathrm{RF}})t} + \mathbf{n}_0(t)\\ =& \mathbf{E}_{C0}e^{j\omega_0 t}\left(1+\alpha e^{j\omega_{\mathrm{RF}}t}\sum_{k=-\frac{1}{2}N_{sc}+1}^{\frac{1}{2}N_{sc}} c_k e^{j\omega_k t}\right) + \mathbf{n}_0(t)\end{aligned} \tag{1}$$

where $f_0 = \omega_0/2\pi$ is the frequency of the main optical carrier, and $f_{\mathrm{RF}} = \omega_{\mathrm{RF}}/2\pi$ is the frequency offset between the baseband optical OFDM signal and the optical carrier. $\mathbf{E_{C0}}$ and $\mathbf{E_{S0}}$ are the lightwave field amplitude of the optical carrier and optical OFDM signal, respectively, and we assume they have the same polarization state, viz., $\mathbf{E_{C0}}//\mathbf{E_{S0}}$. $s_B(t) = \sum_{k=-(1/2)N_{sc}+1}^{(1/2)N_{sc}} c_k e^{j\omega_k t}$ is the normalized baseband OFDM signal in electrical domain and $\sum |c_k|^2 = 1$; c_k and $f_k = \omega_k/2\pi = kB/N_{sc} = k/T$ represent the kth complex signal information and its subcarriers frequency of the OFDM signal with N_{sc} subcarriers and the symbol duration of T, respectively. B is the bandwidth of the OFDM signal. Here, for the sake of mathematical simplicity, only one OFDM symbol is considered. $\mathbf{n}_0(t)$ is the optical electrical field of the noise associated with the SSB-OOFDM signal on both polarization directions in time domain.

If the optical launch power is not too high, the fiber nonlinearity remains sufficiently low and thus the optical fiber link can be modeled as a linear channel [26]. Hence, the optical signal and noise can be assumed independent. After transmitted over the fiber link, the received noised SSB-OOFDM signal is approximately expressed as

$$\begin{aligned}\mathbf{E}_R(t) =& \beta\mathbf{E}_{C0}\left\{e^{j[\omega_0 t+\varphi(t)]} + \alpha\sum_{k=-\frac{1}{2}N_{sc}+1}^{\frac{1}{2}N_{sc}} c_k e^{j[(\omega_0+\omega_{\mathrm{RF}}+\omega_k)t+\varphi_k(t)]}\right\} + \mathbf{n}(t)\\ \propto& \mathbf{E}_C e^{j[\omega_0 t+\varphi(t)]}\left(1+\alpha e^{j\omega_{\mathrm{RF}}t}\sum_{k=-\frac{1}{2}N_{sc}+1}^{\frac{1}{2}N_{sc}} c_k e^{j\omega_k t}\right) + \mathbf{n}(t).\end{aligned} \tag{2}$$

Here, to simplify the analysis, the transmission loss β is ignored and the phase shift of the subcarriers is approximated as $\varphi(t)$, which is proper if the transmission distance is not too long. $\mathbf{n}(t)$ denotes the received noise optical electrical field in the horizontal and vertical polarizations, $n_h(t)$ and $n_v(t)$, respectively. The optical noise is assumed unpolarized (statistically equal power in both polarizations) and is band-limited by an optical filter (B_m), extending from B_L below the carrier (f_0) to B_H above it in frequency domain. $B_m = B_H + B_L$ is the total optical noise bandwidth, as depicted in Fig. 1. The noised SSB-OOFDM signal model in our analysis is based on [10], [23], but here we mainly analyze the influence of the SSBI as well as other noise on the received OFDM signal with the GB smaller than the bandwidth of the OFDM signal. Assume that the whole SSB- OOFDM is sent on the horizontal polarization. We define $\alpha \equiv |\mathbf{E}_S|/|\mathbf{E}_C| = E_S/E_C = 1/\sqrt{\mathrm{CSR}}$ [9], and so the total optical power of the received SSB-OOFDM signal is $P_O = |\mathbf{E}_C|^2 + |\mathbf{E}_S|^2 = (1+\alpha^2)E_C^2$. The power spectral density of the optical noise $p_N(\omega)$ is

$$p_N(\omega) = |\mathbb{F}\{\mathbf{n}(t)\}|^2 \approx p_N \tag{3}$$

$$P_N = \int_{B_m} p_N(\omega)d\omega \approx 2\pi p_N B_m \tag{4}$$

where $\mathrm{F}\{\cdot\}$ is the Fourier transform, and P_N is the optical noise power in both polarizations integrated over the measurement bandwidth of B_m, which usually is 0.1 nm. Hence, the OSNR can

be defined as

$$\mathrm{OSNR} = \frac{P_O}{P_N} = \frac{(1+\alpha^2)E_C^2}{2\pi p_N B_m}. \tag{5}$$

Using an optical filter and a square-law photodiode, we obtain the photocurrent by direct detection

$$\begin{aligned}
I(t) &\propto \mu|\mathbf{E}_R(t)|^2 + w(t) \\
&= \mu\left|\mathbf{E}_C e^{j\omega_0 t}\left(1+\alpha e^{j\omega_{\mathrm{RF}}t}\sum_{k=-\frac{1}{2}N_{sc}+1}^{\frac{1}{2}N_{sc}} c_k e^{j\omega_k t}\right) + n_h(t)\right|^2 + \mu|n_v(t)|^2 + w(t) \\
&= \mu E_C^2 + \mu\alpha^2 E_C^2 \sum_{k,k'=-\frac{1}{2}N_{sc}+1}^{\frac{1}{2}N_{sc}} c_k c_{k'}^* e^{j(\omega_k-\omega_{k'})t} + \mu|n_h(t)|^2 + \mu|n_v(t)|^2 + w(t) \\
&\quad + \mu\alpha E_C \sum_{k=-\frac{1}{2}N_{sc}+1}^{\frac{1}{2}N_{sc}} \left[c_k e^{j(\omega_{\mathrm{RF}}+\omega_k)t} + c_k^* e^{-j(\omega_{\mathrm{RF}}+\omega_k)t}\right] + \mu E_C\left[n_h^*(t)e^{j\omega_0 t} + n_h(t)e^{-j\omega_0 t}\right] \\
&\quad + \mu E_C\alpha\left[e^{j(\omega_0+\omega_{\mathrm{RF}})t}\sum_{k=-\frac{1}{2}N_{sc}+1}^{\frac{1}{2}N_{sc}} c_k e^{j\omega_k t} n_h^*(t) + e^{-j(\omega_0+\omega_{\mathrm{RF}})t}\sum_{k=-\frac{1}{2}N_{sc}+1}^{\frac{1}{2}N_{sc}} c_k^* e^{-j\omega_k t} n_h(t)\right] + w(t) \\
&= \underbrace{\mu E_C^2}_{DC} + \underbrace{2\mu\alpha E_C^2 \mathrm{Re}\left\{e^{j\omega_{\mathrm{RF}}t}\sum_{k=-\frac{1}{2}N_{sc}+1}^{\frac{1}{2}N_{sc}} c_k e^{j\omega_k t}\right\}}_{(a)} + \underbrace{\mu\alpha^2 E_C^2 \sum_{k,k'=-\frac{1}{2}N_{sc}+1}^{\frac{1}{2}N_{sc}} c_k c_{k'}^* e^{j(\omega_k-\omega_{k'})t}}_{(b)} \\
&\quad + \underbrace{2\mu E_C \mathrm{Re}\left[n_h^*(t)e^{j\omega_0 t}\right]}_{(c)} + \underbrace{2\mu\alpha E_C \mathrm{Re}\left[n_h^*(t)e^{j(\omega_0+\omega_{\mathrm{RF}})t}\sum_{k=-\frac{1}{2}N_{sc}+1}^{\frac{1}{2}N_{sc}} c_k e^{j\omega_k t}\right]}_{(d)} \\
&\quad + \underbrace{\mu\left[|n_h(t)|^2 + |n_v(t)|^2\right]}_{(e)} + w(t)
\end{aligned} \tag{6}$$

where μ is the photodiode responsivity, $\mathrm{Re}[x]$ takes the real part of x, and * denotes the complex conjugator. Term (a) is the desired OFDM signal, viz., the beating between the main carrier and the subcarriers, as shown in Fig. 1(a); term (b) is the beating between the subcarriers which is SSBI, as shown in Fig. 1(b); term (c), (d), and (e) are the beatings of the main carrier and optical noise (C-noise), optical OFDM signal and optical noise (S-noise), and optical noise and optical noise (noise-noise), respectively, as shown in Fig. 1(c), (d), and (e); the first term E_C^2 is the self-beating of the optical carrier, and is the DC component of the photocurrent. The last term $w(t)$ denotes the shot and thermal noise generated by the PD. In order to further investigate the influence of SSBI, its photocurrent is further expressed as

$$\begin{aligned}
n_{\mathrm{SSBI}}(t) &= \mu\alpha^2 E_C^2 \sum_{k,k'=-\frac{1}{2}N_{sc}+1}^{\frac{1}{2}N_{sc}} c_k c_{k'}^* e^{j(\omega_k-\omega_{k'})t} = \mu\alpha^2 E_C^2 \sum_{k,k'=-\frac{1}{2}N_{sc}+1}^{\frac{1}{2}N_{sc}} c_k c_{k'}^* e^{j(k-k')2\Delta\omega t} \\
&= \mu\alpha^2 E_C^2 \sum_{p=-N_{sc}+1}^{N_{sc}-1}\left(\sum_{k=-\frac{1}{2}N_{sc}+1}^{\frac{1}{2}N_{sc}} c_k c_{k-p}^* e^{jp\Delta\omega t}\right) \\
&= \mu\alpha^2 E_C^2\left(\sum_{k=-\frac{1}{2}N_{sc}+1}^{\frac{1}{2}N_{sc}}|c_k|^2 + 2\sum_{p=1}^{N_{sc}-1}\sum_{k=-\frac{1}{2}N_{sc}+1}^{\frac{1}{2}N_{sc}-p}\mathrm{Re}\left\{c_{k+p}c_k^* e^{jp\Delta\omega t}\right\}\right) = \mu\frac{\alpha^2}{1+\alpha^2}P_O\left(A_0 + 2\sum_{p=1}^{N_{sc}-1}A_p\right)
\end{aligned} \tag{7}$$

where $A_p = \sum_{k=-(1/2)N_{sc}+1}^{(1/2)N_{sc}-p} \mathrm{Re}\{c_{k+p}c_k^* e^{jp\Delta\omega t}\}$ $(p = 0, 1, 2, \ldots, N_{sc}-1)$, $\Delta\omega = 2\pi\Delta f = 2\pi/T$ is the frequency spacing between subcarriers, and $B = N_{sc}/T = N_{sc}\cdot\Delta f$. According to the statistical average, A_p reduces linearly as p increases. That means the power spectrum of SSBI has a triangle outline, and distributes from 0 to B, as shown in Fig. 1(b).

From Fig. 1, it can be seen that the desired OFDM signal is distributed from $f_{\mathrm{RF}} + f_{-(1/2)N_{SC}+1}$ to $f_{\mathrm{RF}} + f_{(1/2)N_{SC}+1}$ in the frequency domain, viz., $[\mathrm{GB}, \mathrm{GB}+B]$, while the main interference, SSBI, with the raw frequency range $[0, B]$, will overlap with the desired OFDM signal if $\mathrm{GB} < B$. Here we only consider this case for pursuing a higher SE. After the opto-electrical conversion, an EBF with the bandwidth of B_e is used to suppress the outband SSBI, and so the remaining SSBI photocurrent along with the OFDM signal can be given as

$$n'_{\mathrm{SSBI}}(t) = 2\mu\alpha^2 E_C^2 \sum_{p=N_G}^{N_{sc}-1} \sum_{k=-\frac{1}{2}N_{sc}+1}^{\frac{1}{2}N_{sc}-p} \mathrm{Re}\{c_{k+p}c_k^* e^{jp\Delta\omega t}\} = 2\mu\alpha^2 E_C^2 \sum_{p=N_G}^{N_{sc}-1} A_p \tag{8}$$

where $N_G = \lfloor (N_{sc}/B)(\mathrm{GB}-B) \rfloor$. Thus, the power of SSBI, i.e., P_{SSBI}, after the EBF can be expressed as

$$\begin{aligned} P_{\mathrm{SSBI}} &= R\left(2\mu\frac{\alpha^2}{1+\alpha^2}P_O\right)^2 \left[\sum_{k=N_G+1}^{N_{sc}-1} A_p^2\right] = \frac{4R\mu^2\alpha^4}{(1+\alpha^2)^2}P_O^2 \sum_{k=N_G+1}^{N_{sc}-1} \left[\left(\sum |c_k|^2\right)\frac{N_{sc}-k}{N_{sc}}\right]^2 \\ &= \frac{R\mu^2\alpha^4}{(1+\alpha^2)^2}\frac{P_O^2}{6}N_{sc}\left[\left(1+\frac{B_e}{B}-2\frac{\mathrm{GB}}{B}\right)-\frac{2}{N_{sc}}\right]\left[\left(1+\frac{B_e}{B}-2\frac{\mathrm{GB}}{B}\right)-\frac{1}{N_{sc}}\right]\left(1+\frac{B_e}{B}-2\frac{\mathrm{GB}}{B}\right) \end{aligned} \tag{9}$$

where R is the load resistance. The power calculation of the photocurrent is $P = I^2R(R+r)^{-2}r^2$, here r is the photodiode resistance. Since the factor $(R+r)^{-2}r^2$ is a constant for the power calculation of the signal, interference and all the noises, we neglected the factor to simplify the expression, namely, in the calculation of the signal, interference and noise power below, their powers are expressed as $P = I^2R$. It can be seen from (9) that the remaining SSBI depends on the CSR $(1/\alpha)$ and the GB of the SSB-OOFDM signal, but its influence on the received OFDM signal is also trimmed by the EBF.

The power of the received OFDM signal P_S can be expressed as

$$P_S = R\left(2\mu\alpha E_C^2\right)^2 \sum |c_k|^2 = 4R\mu^2\alpha^2 E_C^4 = 4R\mu^2 \frac{\alpha^2}{(1+\alpha^2)^2} P_O^2. \tag{10}$$

Here, it can be observed that if the launch optical power P_O is constant, the OFDM signal with CSR = 0 dB $(\alpha = 1)$ produces the maximal electrical OFDM signal in the photocurrent, and thus the optimal sensitivity of the receiver if the interference and noises are not considered. However, the optical noises degrade the desired OFDM signal and make the condition different in addition to the SSBI. According to (6), the noises after opto-electrical conversion and trimmed by EBF can be approximately expressed as

$$P_{C-\mathrm{noise}} = R\left\{2\mu E_C \mathrm{Re}\left[n_h^*(t)e^{j\omega_0 t}\right]\right\}^2 \approx 8\pi R\mu^2 E_C^2 p_N B_e = \frac{4R\mu^2}{1+\alpha^2}P_O^2\frac{B_e}{\mathrm{OSNR}\cdot B_m} \tag{11}$$

$$\begin{aligned} P_{S-\mathrm{noise}} &= R\left\{2\mu\alpha E_C \mathrm{Re}\left[n_h^*(t)e^{j(\omega_0+\omega_{\mathrm{RF}})t}\sum_{k=-\frac{1}{2}N_{sc}+1}^{\frac{1}{2}N_{sc}} c_k e^{j\omega_k t}\right]\right\}^2 \approx 8\pi R\mu^2\alpha^2 E_C^2 p_N B_e \\ &= \frac{4R\mu^2\alpha^2}{1+\alpha^2}P_O^2\frac{B_e}{\mathrm{OSNR}\cdot B_m} \end{aligned} \tag{12}$$

$$P_{\mathrm{noise}-\mathrm{noise}} = R\left\{\mu\left[|n_h(t)|^2 + |n_v(t)|^2\right]\right\}^2 \approx 16\pi^2\mu^2 p_N^2 R B_e^2 = 4R\mu^2 P_O^2 \frac{B_e^2}{\mathrm{OSNR}^2\cdot B_m^2}. \tag{13}$$

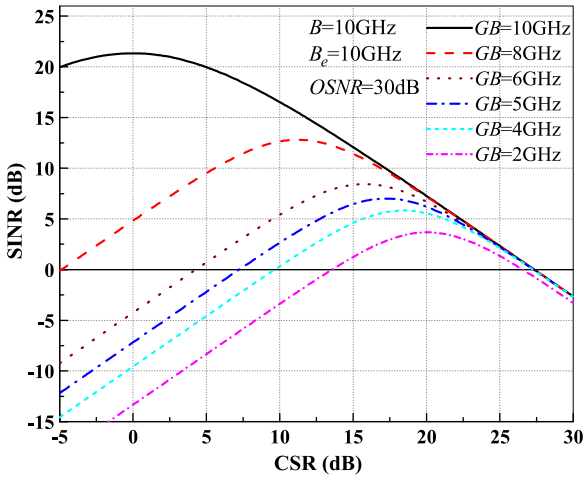

Fig. 2. SINR as the function of CSR for the SSB-OOFDM signal with different GBs.

In addition, the powers of the shot and thermal noise of the PD in the resistive matched case, which are denoted by $w(t)$ in the photocurrent of (6), can be expressed as [27]

$$P_w = P_{\text{shot}} + P_{th} \tag{14}$$
$$P_{\text{shot}} = 2e[\langle I(t)\rangle + I_d]B_eR = 2e(\mu P_O + I_d)B_eR \tag{15}$$
$$P_{th} = 4k_BT_kB_e \tag{16}$$

where P_{shot}, P_{th} are the power of shot and thermal noise of PD, respectively; $I(t)$ has been given as (6); I_d is the dark current of the PD, and k_B, e, and T_k are Boltzmann constant, the electron charge, and Kelvin temperature, respectively. Therefore, the total noise power P_{noise} can be expressed as

$$\begin{aligned} P_{\text{noise}} &= P_{C-\text{noise}} + P_{S-\text{noise}} + P_{\text{noise}-\text{noise}} + P_{\text{shot}} + P_{th} \\ &= 4R\mu^2P_O^2\frac{B_e}{\text{OSNR}\cdot B_m} + 4R\mu^2P_O^2\frac{B_e^2}{\text{OSNR}^2\cdot B_m^2} + (2\mu ReP_O + 2ReI_d + 4k_BT_k)B_e. \end{aligned} \tag{17}$$

Therefore, the SINR, which is inversely proportional to EVM, can be expressed as

$$\text{SINR} = \frac{P_S}{P_{\text{SSBI}} + P_{\text{noise}}} \tag{18}$$

and

$$\begin{aligned} \frac{1}{\text{SINR}} = \frac{N_{sc}\alpha^2}{24}&\left[\left(1+\frac{B_e}{B}-2\frac{\text{GB}}{B}\right)-\frac{2}{N_{sc}}\right]\left[\left(1+\frac{B_e}{B}-2\frac{\text{GB}}{B}\right)-\frac{1}{N_{sc}}\right]\left(1+\frac{B_e}{B}-2\frac{\text{GB}}{B}\right) \\ &+\left(\alpha+\frac{1}{\alpha}\right)^2\left[\left(\frac{B_e}{\text{OSNR}^2\cdot B_m^2}+\frac{1}{\text{OSNR}\cdot B_m}+\frac{e}{2\mu P_O}\right)+\frac{1}{\mu^2P_O^2}\left(\frac{eI_d}{2}+\frac{k_BT_k}{R}\right)\right]B_e. \end{aligned} \tag{19}$$

It can be seen that SINR depends on the GB, CSR, and B_e, as well as the OSNR of the received SSB-OOFDM signal. The EBF and the PD at the receiver also have impact on the signal performance. In the ideal case with $B_e = B$, which means an ideal matched electrical filter is used, the SSBI power depends on GB completely. If $B_e > B$, the EBF leaks more noise; otherwise, it trims the OFDM signal and degrades the performance seriously. Here the 40 Gb/s 16-QAM SSB-OOFDM signal is considered with the subcarrier number of $N_{sc} = 128$, the optical power of $P_O = -0.7$ dBm, the photodiode responsivity of $\mu = 1$ A/W, the dark current of $I_d = 10$ nA, load

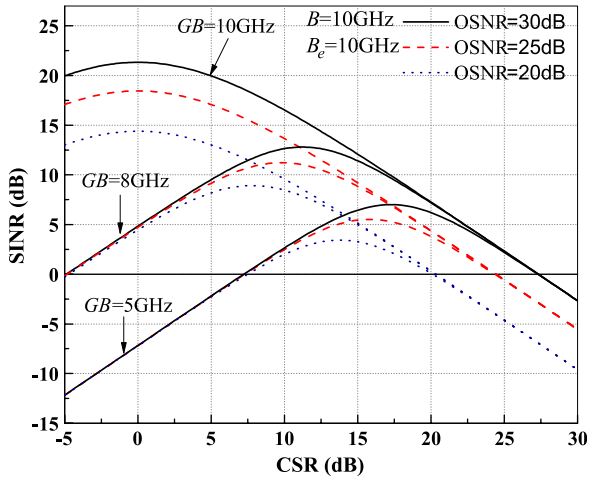

Fig. 3. SINR as the function of CSR for different OSNRs at GB = 5, 8, and 10 GHz.

resistance of $R = 1\ \Omega$, and $B_m = 0.1$ nm at the temperature of $T_k = 300$ K. The SINR versus the CSR of the SSB-OOFDM signal at different GBs with $B_e = B = 10$ GHz and OSNR = 30 dB is given in Fig. 2.

From Fig. 2, it can be seen that for the SSB-OOFDM signal with GB = 10 GHz, the highest maximum SINR of 21.5 dB is obtained at the optimum CSR of 0 dB, which agrees with [1]. However, the optimum CSR increases to 11, 15.5 and 17 dB for GB = 8, 6 and 5 GHz, respectively, and correspondingly, the maximum SINR is reduced to 12.7, 8.7, and 6.9 dB. At the left of the optimum CSR, the SINR increases as CSR increases. For instance, for the case of GB = 8 GHz, the SINR at CSR = 11 dB is 10 dB better than that of CSR = 0 dB. The decreased maximum SINR attributes to the fact that more SSBI are overlapped with the OFDM signal at the smaller GB.

On the other hand, for a given total optical power and fixed GB of the SSB-OOFDM signal, as the CSR increases, the SSBI reduces faster than the desired OFDM signal and so the SINR increases firstly. While, if the CSR increases further, the SINR decreases inversely as the optical noise and transmission distortions become dominant. Therefore, there exists an optimum CSR where the SSBI and the optical noise are balanced. Moreover, the optimum CSR increases as the GB reduces since the more SSBI demands a higher CSR to balance. It means that a certain increased CSR can suppress the degradation caused by the SSBI for the SSB-OOFDM signal with a fixed GB. The SINR at GB = 6 GHz and CSR = 15 dB is almost equal to the case at GB = 8 GHz and CSR = 3 dB. Therefore, there exists a tradeoff between CSR and GB, which means that the degradation caused by the reduced GB at higher CSR can be compensated for by the increased GB at lower CSR. Of course, as CSR > 25 dB, the influence of the GB on the SINR becomes minor since the SSBI becomes much smaller compared with the desired OFDM signal.

To further investigate the influence of the OSNR of the SSB-OOFDM signal on the optimum CSR, the SINR versus the CSR with $B_e = B = 10$ GHz for different OSNRs at the GB = 5, 8 and 10 GHz is shown in Fig. 3. The optimum CSR keeps still 0 dB as the OSNR increases for the SSB-OOFDM signal with GB = 10 GHz since the spectrum overlapping of the SSBI and the desired OFDM signal is avoided. However, if GB < 10 GHz, the optimum CSR increases with the OSNR increasing. It can be seen that the optimum CSR increases about 4 dB as OSNR increases from 20 dB to 30 dB for GB = 8 and 5 GHz. This is because the optical noises at higher OSNR are smaller than the received OFDM signal, and the optical noises have less influence on the tradeoff between SSBI and optical noises at higher CSR. It is worth noting that as GB < B, the SINR is becoming sensitive to the GB but insensitive to OSNR as the CSR is smaller than the optimal value, vice versa, according to Fig. 3. The OSNR has little influence on the SINR of the received OFDM signal for the case with the CSR < 10 dB at GB = 5 GHz and that with the

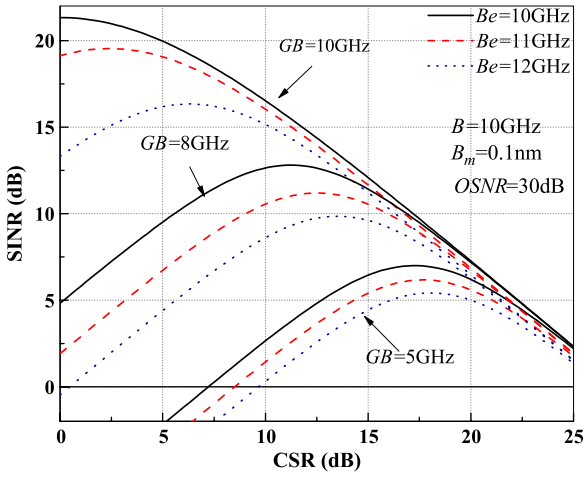

Fig. 4. SINR as the function of CSR as different B_e at GB = 5, 8, and 10 GHz.

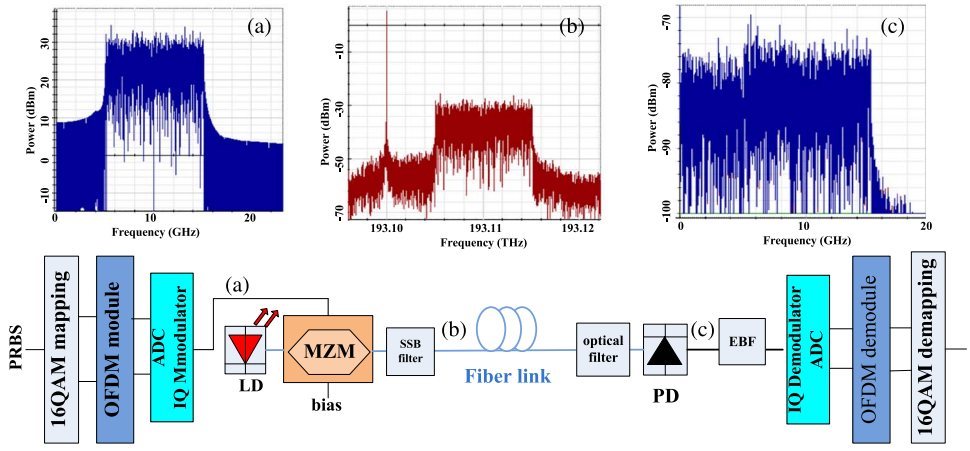

Fig. 5. Simulation link of the direct-detection SSB-OOFDM. (a) Spectrum of RF-OFDM signal. (b) Spectra of the transmitted RF-OFDM. (c) Received RF-OFDM signal.

CSR < 5 dB at GB = 8 GHz since the SSBI distortion is domain in comparison with the optical noise, and has great difference for GB = 5 GHz and 8 GHz. However, when CSR > 20 dB, the SINR is independence of the GB but shows obviously difference at different OSNRs since the impact of the optical noise of the SSB-OOFDM signal is dominant in compared with the SSBI.

The EBF with the bandwidth of B_e, which suppresses the out-of-band SSBI and other noises in the photocurrent, also varies the optimum CSR as $B_e \geq B$. Fig. 4 shows the SINR versus the CSR of the SSB-OOFDM signal with GB = 5, 8 and 10 GHz as B_e = 10, 11, and 12 GHz. It can be seen that B_e has more influence on the optimum CSR as GB = 10 GHz since the increase of B_e introduces more out-of-band SSBI to interfere the OFDM signal. Thus, the optimum CSR increases from 0 dB to 2.1 dB and to 6.2 dB as B_e increases from 10 GHz to 11 GHz and to 12 GHz, respectively. However, for the case of GB smaller than B, the optimum CSR increases slowly with B_e. For example, it increases only about 2 dB and 1 dB as B_e increases from 10 GHz to 12 GHz for the cases of GB = 8 GHz and 5 GHz, respectively. This can be illustrated as that a larger B_e introduces more leaked SSBI and optical noises simultaneously, while the impact of SSBI is larger than the optical noises. Therefore, a little larger optimum CSR is required to suppress the SSBI. GB = 10 GHz and GB < 10 GHz have two different effects on the CSR as OSNR and B_e vary, and two cases of OSNR and B_e would be investigated in our following simulation.

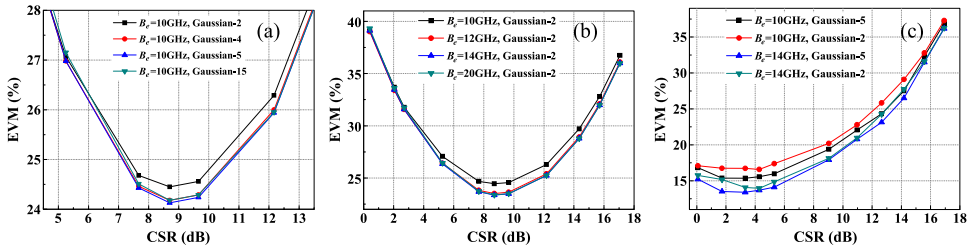

Fig. 6. EVM as a function of EBF with different B_e and orders for the SSB-OOFDM signal at OSNR = 22 dB. (a) EVM versus CSR with different orders EBF at B_e = 10 GHz and with GB = 5 GHz. (b) EVM versus CSR with the second-order. Gaussian EBF at different B_e with GB = 5 GHz. (c) EVM versus CSR with different orders and B_e of EBF at GB = 10 GHz.

3. Simulation Setup and Results

To verify our theoretical results above, a direct-detection SSB-OOFDM system is built based on the simulation platform. The system consists of the optical OFDM transmitter, fiber transmission link and the optical OFDM receiver, as depicted in Fig. 5. First, a 40 Gb/s pseudo-random bit sequence (PRBS) is mapped into 16-QAM symbol serial and is then put into OFDM module for serial-parallel conversion and IFFT and parallel-serial conversion. Here, the IFFT size is 256. Among the 256 subcarriers, 128 subcarriers are allocated for bearing the signals, whereas the others are zero-padded at the edges for oversampling. No cyclic prefix is added because the chromatic dispersion is small for the short fiber length considered. Second, after DAC, the baseband OFDM signal is upconverted by the IQ modulator with the RF frequency varying from 10 to 15 GHz for observing the influence of the GB on the system performance. The 10 GHz RF-OFDM signal with GB = 5 GHz is shown by the spectrum in Fig. 5(a). Third, in the optical OFDM systems, to reduce the MZM nonlinearity, the RF-OFDM signal with the a peak-to-peak voltage swing of $0.5V_{\pi}$ is used to drive the arms of MZM in a pull-push pattern to modulate the lightwave from a CW laser diode with the central wavelength of 193.1 THz and the linewidth of 0.1 MHz. The DSB-OOFDM signal is generated and the SSB-OOFDM signal is obtained by SSB filtering. The CSR can be adjusted flexibly by tuning the dc bias voltage of MZM and the attenuator. The optical spectrum of SSB-OOFDM signal with the GB of 5 GHz and CSR of 0.4 dB is shown in Fig. 5(b) with the OSNR of the SSB-OOFDM signal of 30 dB/0.1 nm, and the OSNR can be adjusted by a white light source along with an optical amplifier. Here, the launch power is kept at 6 dBm, which is small enough to avoid the fiber nonlinearity.

The SSB-OOFDM signal is transmitted through a 20 km standard single mode fiber (SSMF) with the power loss of 0.2 dB/km and dispersion of 16 ps/nm·km, and then it is directly injected into the PD with 1 A/W responsivity and thermal noise of 10^{-22} W/Hz to the electrical one. Since the wall-off time between the two most outside subcarriers is $20\ \text{km} \times 0.08\ \text{nm} \times 16\ \text{ps/nm} \cdot \text{km} = 2.56$ ps and is much smaller the sampling period of 50 ps, we do not introduce cyclic prefix in the simulation. Fig. 5(c) shows the RF spectrum of the received OFDM signal from the SSB-OOFDM signal with the GB of 5 GHz and CSR of 0.4dB. After passing through the Gaussian EBF with different bandwidth of B_e, the out-of-band noise can be suppressed at different degree. Based on the simulation, the EBF is optimized to minimize distortion of the OFDM signal. At last, following the reverse operations as in the OFDM signal transmitter, including IQ demodulator, ADC, serial-parallel conversion, FFT and parallel-serial conversion, the received OFDM signal is converted back to the 16-QAM digital signal, and the EVM is calculated to quantify the link performance.

Fig. 6 shows the EVM versus CSR curves for the 40 GHz SSB-OOFDM signal with different GB, OSNR and B_e. The simulation is conducted with the Gaussian EBF at different bandwidth of B_e and orders for the received SSB-OOFDM signal with OSNR of 22 dB. The measured EVM as the function of the EBF parameters is firstly investigated. For the case of GB = 5 GHz, the curves of the EVM versus CSR with B_e = 10 GHz at 4th, 5th and 15th orders and with the

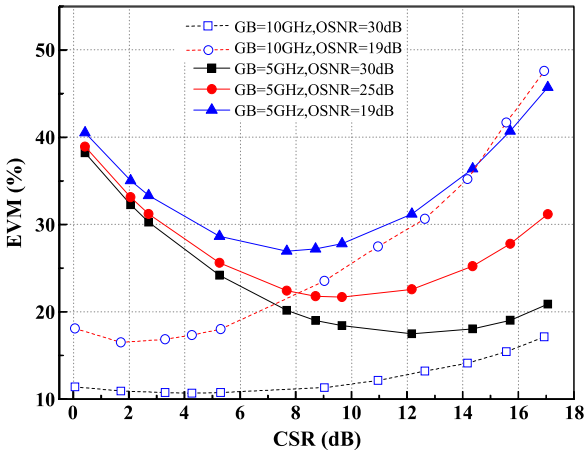

Fig. 7. EVM versus the CSR at different OSNRs for the SSB-OOFDM signal with 14 GHz 5th-order Gaussian EBF at GB = 5 GHz and 10 GHz.

2nd-order EBF at the B_e of 10, 12, 14, 20 GHz are shown in Fig. 6(a) and (b), respectively. At $B_e = 10$ GHz, the EVM decreases as the order of Gaussian EBF increases and reaches a floor at 5th order of Gaussian EBF since the SSBI in band can be completely removed. It can be seen that the optimum CSR exists at 8.7 dB and it does not varies with the bandwidth and orders of the EBF. This agrees with our theoretical result in Fig. 4 that the optimum CSR is not sensitive to B_e as GB = 5 GHz. Specifically, for the 2nd-order Gaussian EBF, as B_e increases from 10 GHz to 20 GHz, the EVM first reduces and then increases slightly, and there exists an optimum bandwidth of $B_e = 14$ GHz, but performance has little difference as $B_e \geq 12$ GHz, as shown in Fig. 6(b). It shows that the relatively large B_e can release the damage. However, as B_e increases from 14 to 20 GHz, the EVM increases gradually since more SSBI and optical noise degrade the signal performance, where the main influence on the received OFDM signal is the CSR rather than the EBF. On the other hand, for the case of GB = 10 GHz, the EVM has similar behavior as that the EVM decreases when B_e increases from 10 GHz to 14 GHz, as shown in Fig. 6(c). But B_e has more influence on the optimum CSR, the optimum CSR at $B_e =$ 14 GHz is 1 dB larger than that of $B_e = 10$ GHz. This is also in accord with the theoretical results in Fig. 4. Hence, to reach the minimum EVM, the 5th-order Gaussian EBF with the bandwidth of 14 GHz is regarded as the optimum and used in following simulations.

Fig. 7 shows the EVMs versus CSR at different GBs and OSNRs for the direct detection receiver with the 5th-order Gaussian EBF at $B_e = 14$ GHz. For the case of GB = 5 GHz, the optimum CSR increases from 7.8 to 10.8 and to 12 dB as the OSNR increases from 20 to 25 and to 30 dB, respectively. This is because a higher OSNR means smaller optical noises to be converted to the electrical ones. So the tradeoff between SSBI and optical noise at a larger CSR is necessary. However, for the case of GB = 10 GHz, the optimum CSR is less sensitive to OSNR, as also demonstrated in Fig. 3.

Fig. 8 shows that the EVMs versus CSR at different GBs with OSNR = 30 dB. It can be seen that the optimal CSR is increased from 4 dB to 9, 11, and 12 dB for SSB-OOFDM signal as the GB reduces from 10 GHz to 8, 6, and 5 GHz, respectively. Correspondingly, the minimal EVM also increases from 10.7% to 11.4%, 14.3%, and 17.5%, respectively. The optimal CSR varies with GB since different GB introduces different SSBI, and therefore, different CSR is required to suppress the SSBI. For the smaller GB, the EVM is worse and a higher optimum CSR is required since the reduced GB introduces a larger SSBI interference. Insets (a) and (b) of Fig. 8 are the constellation diagrams of CSR = 0 dB and CSR = 9 dB at GB = 8 GHz, respectively. For the SSB-OOFDM signal with GB = 10 GHz, the optimum CSR is around 4.3 dB due to the leaked SSBI caused by the increased bandwidth of matched EBF, as shown in the constellation diagram in Fig. 8(c). However, the signal performance degrades as the CSR increases further,

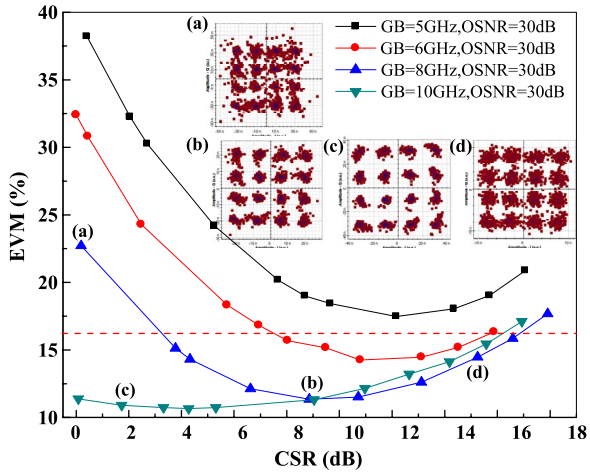

Fig. 8. EVM versus the CSR at different GBs for the SSB-OOFDM signal with 5th-order Gaussian EBF at $B_e = 14$ GHz, and OSNR $= 30$ dB.

which can be seen from the constellation in Fig. 8(d). As the GB reduces, more SSBI contaminates the received OFDM signal, this results in larger optimum CSR and minimal EVM. These agree well with the theoretical prediction by (18) and Fig. 2.

According to the forward error correct (FEC) threshold of the 16 QAM signal of EVM $= 16.3\%$ as the red dashed line in Fig. 8, the SSB-OOFDM signal with CSR $= 8$ dB and GB $= 6$ GHz has the identical EVM with that of CSR $= 3$ dB and GB $= 8$ GHz which can reduce the GB 40% and 20%, respectively. Additionally, the SSB-OOFDM signal with CSR $= 8$ dB and GB $= 8$ GHz also has the identical EVM with that of CSR $= 0$ dB and GB $= 10$ GHz. This indicates that increased CSR can compensate for the EVM caused by the reduced GB, and therefore, the system can achieve the same performance. Therefore, the tradeoff between CSR and GB is required, which achieves higher SE and stable performance by reducing the GB with appropriately increasing CSR in direct-detection SSB-OOFDM system.

4. Conclusion

This paper has theoretically investigated the joint influence of optical CSR and GB on the performance in direct-detection SSB-OOFDM system along with OSNR and EBF. The tradeoff between CSR and GB has been demonstrated by simulations. The performance of direct-detection OFDM system with the GB smaller than B can be improved as the CSR of the optical SSB-OOFDM signal is optimized. The increase of CSR $= 8$ dB can reduce the GB 40%, which improves the SE effectively but without resorting to the complexity of an optical receiver. In addition, the influence of the OSNR and EBF on the system performance is also presented at GB $\leq B$, which can explain the offset of the optimum CSR in different situations. It shows that the optimum CSR is more sensitive to OSNR at GB $< B$ than that at GB $= B$. However, the optimum CSR at GB $< B$ is less sensitive to B_e than that at GB $= B$. In all, the analysis of these effect factors provides a deep insight on both reducing the SSBI and improving the SE in direct-detection SSB-OOFDM system.

References

[1] A. J. Lowery, L. B. Du, and J. Armstrong, "Performance of optical OFDM in ultralong-haul WDM lightwave systems," *J. Lightw. Technol.*, vol. 25, no. 1, pp. 131–138, Jan. 2007.
[2] B. Schmidt, Z. Zan, L. B. Du, and A. J. Lowery, "100 Gbit/s transmission using single-band direct-detection optical OFDM," presented at the Opt. Fiber Commun. Conf., San Diego, CA, USA, Mar. 22–26, 2009, Paper PDPC3.
[3] Y. Hong, A. J. Lowery, and E. Viterbo, "Sensitivity improvement and carrier power reduction in direct-detection optical OFDM systems by subcarrier pairing," *Opt. Exp.*, vol. 20, no. 2, pp. 1635–48, Jan. 2012.

[4] J. Ma, "Simple signal-to-signal beat interference cancellation receiver based on balanced detection for a single-sideband optical OFDM signal with a reduced guard band," *Opt. Lett.*, vol. 38, no. 21, pp. 4335–4338, Nov. 2013.
[5] F. Li, X. Li, J. Yu, and L. Chen, "Optimization of training sequence for DFT-spread DMT signal in optical access network with direct detection utilizing DML," *Opt. Exp.*, vol. 22, no. 19, pp. 22 962–22 967, Sep. 2014.
[6] F. Li *et al.*, "High-level QAM OFDM system using DML for low-cost short reach optical communications," *IEEE Photon. Technol. Lett.*, vol. 26, no. 9, pp. 941–944, May 2014.
[7] Z. Cao *et al.*, "Reduction of intersubcarrier interference and frequency-selective fading in OFDM-ROF systems," *J. Lightw. Technol.*, vol. 28, no. 16, pp. 2423–2429, Aug. 2010.
[8] Z. Cao, J. Yu, W. Wang, L. Chen, and Z. Dong, "Direct-detection optical OFDM transmission system without frequency guard band," *IEEE Photon. Technol. Lett.*, vol. 22, vol. 11, pp. 736–738, Jun. 2010.
[9] P. Yang, S. Hu, and X. Chen, "A novel algorithm for SSBI mitigation in a DD-SSB-OFDM transmission system," presented at the Asia Commun. Photonics Conf., OSA, Beijing, China, Nov. 12–15, 2013, Paper AW3F.4.
[10] A. J. Lowery, "Improving sensitivity and spectral efficiency in direct-detection optical OFDM systems," presented at the Optical Fiber Commun. Conf., San Diego, CA, USA, Feb. 24–28, 2008, Paper OMM4.
[11] A. J. Lowery, "Amplified-spontaneous noise limit of optical OFDM lightwave systems," *Opt. Exp.*, vol. 16, no. 2, pp. 860–865, Jan. 2008.
[12] G. Wen *et al.*, "Experimental investigation of pilot power allocation in direct-detected optical orthogonal frequency division multiplexing system," *Opt. Eng.*, vol. 52, no. 1, 2013, Art ID. 015009.
[13] Q. Tang *et al.*, "Joint adaptive code rate technique and bit interleaver for direct-detection optical OFDM system," *Opt. Fiber Technol.*, vol. 19, no. 1, pp. 35–39, Jan. 2013.
[14] F. Li, J. Yu, J. Xiao, Z. Cao, and L. Chen, "Reduction of frequency fading and imperfect frequency response with pre-emphasis technique in OFDM-ROF systems," *Opt. Commun.*, vol. 284, no. 19, pp. 4699–4705, Sep. 2011.
[15] Y. Gao *et al.*, "Direct-detection optical OFDM transmission system with pre-emphasis technique," *J. Lightw. Technol.*, vol. 29, no. 14, pp. 2138–2145, Jul. 2011.
[16] Z. Cao *et al.*, "Unbalanced impairments compensation for low cost direct detection OFDM-PON systems," *Opt. Commun.*, vol. 310, pp. 35–41, Jan. 2014.
[17] Z. Cao, G. Wen, L. Chen, Q. Shu, and L. Chen, "Comparison of interpolation methods for pilot aided estimation in direct-detection optical OFDM system," *Microw. Opt. Technol. Lett.*, vol. 55, no. 11, pp. 2604–2608, Nov. 2013.
[18] I. N. Cano, M. C. Santos, and J. Prat, "Optimum carrier to signal power ratio for remote heterodyne DD-OFDM in PONs," *IEEE Photon. Technol. Lett.*, vol. 25, no. 13, pp. 1242–1245, Jul. 2013.
[19] C. Zizheng, L. Zou, C. Lin, and Y. Jianjun, "Impairment mitigation for a 60 GHz OFDM radio-over-fiber system through an adaptive modulation technique," *IEEE/OSA J. Opt. Commun. Netw.*, vol. 3, no. 9, pp. 758–766, Sep. 2011.
[20] X. Wang, J. Yu, Z. Cao, J. Xiao, and L. Chen, "SSBI mitigation at 60 GHz OFDM-ROF system based on optimization of training sequence," *Opt. Exp.*, vol. 19, no. 9, pp. 8839–8846, Apr. 2011.
[21] L. Fan, C. Zizheng, L. Xinying, and C. Lin, "SSMI cancellation in direct-detection optical OFDM with novel half-cycled OFDM," in *Proc. 39th ECOC*, 2013, pp. 1–3.
[22] W. R. Peng, I. Morita, and H. Tanaka, "Enabling high capacity direct-detection optical OFDM transmissions using beat interference cancellation receiver," presented at the Eur. Conf. Exh. Opt. Commun., Torino, Italy, Sep. 19–23, 2010, Paper Tu.4.A.2.
[23] W. R. Peng *et al.*, "Theoretical and experimental investigations of direct-detected RF-tone-assisted optical OFDM systems," *J. Lightw. Technol.*, vol. 27, no. 10, pp. 1332–1339, May 2009.
[24] S. L. Jansen, I. Morita, and H. Tanaka, "Carrier-to-signal power in fiber-optic SSB-OFDM transmission systems," in *Proc. IEICE Gen. Conf.*, 2007, p. 363, Paper B-10-24.
[25] A. Abdulamir, L. Jochen, and R. Werner, "Spectral efficiency and receiver sensitivity in direct detection optical-OFDM," presented at the Opt. Fiber Commun. Conf., San Diego, CA, USA, Mar. 22–26, 2009, Paper OMT7.
[26] S. A. Nezamalhosseini *et al.*, "Theoretical and experimental investigation of direct detection optical OFDM transmission using beat interference cancellation receiver," *Opt. Exp.*, vol. 21, no. 13, pp. 15 237–15 246, 2013.
[27] H. Al-Raweshidy and S. Komaki, *Radios Over Fiber Technologies for Mobile Communications Network*. Norwood, MA, USA: Artech House, 2002.